Available online at www.sciencedirect.com
SCIENCE DIRECT®
Applied Thermal Engineering 26 (2006) 663–672
APPLIED THERMAL ENGINEERING
www.elsevier.com/locate/apthermeng

Modelling and hourly simulation of a solar ejector cooling system

Humberto Vidal [a,*], Sergio Colle [b,1], Guilherme dos Santos Pereira [b,1]

[a] Department of Mechanical Engineering, University of Magallanes, P.O. Box 113-D Punta Arenas, Chile
[b] LABSOLAR—Department of Mechanical Engineering, Federal University of Santa Catarina, 88040-900 Florianópolis, SC, Brazil

Received 17 January 2005; accepted 8 September 2005
Available online 2 November 2005

Abstract

This paper deals with the hourly simulation of an ejector cooling cycle assisted by solar energy. The system is simulated using the TRNSYS program and the typical meteorological year (TMY) file that contains the weather data from Florianópolis, Brazil. The ejector cycle uses R141b as the working fluid and a one-dimensional ejector is modelled in EES (Engineering Equation Solver). A cooling capacity of 10.5 kW is considered and a parametric optimization is carried out to select the optimum size of the system. Simulation results show the auxiliary energy usage and the useful heat gain for different types and areas of solar collector. Additionally, the effect on energy usage of storage tank, collector slope angle and hot water flow rate is studied. The optimized system consists of 80 m^2 of flat plate collector tilted 22° from the horizontal, a 4 m^3 hot water storage tank and a mass ratio equal to 8.

Keywords: Ejector; Hourly simulation; Cooling; Refrigeration; Solar

1. Introduction

The solar-driven ejector refrigeration system appears as an attractive alternative for refrigeration technologies due to its capacity to use low temperature heat supply. Its major components include solar collectors, a hot water storage tank, an ejector cycle and an auxiliary pre-heater as shown in Fig. 1. The collector pump circulates water between the collector and the storage tank. The water conveys heat from the collector to the storage tank. Then, hot water from the storage tank is carried to the generator where the refrigerant vaporizes. When the heat provided by the storage tank is not sufficient, the auxiliary pre-heater acts as an additional source of energy to ensure that pressure and temperature conditions required by the ejector are achieved. The high pressure primary vapor flow is generated and the low pressure vapor flow of the refrigerant coming from the evaporator is induced to the ejector. The primary and the secondary vapor stream are mixed at the mixing section where an aerodynamic shock is induced to create a compression effect. The mixed stream is then discharged, via a diffuser, to a condenser rejecting heat at ambient temperature to the cooling water system. Then, the refrigerant flows through an expansion valve to the evaporator, where it absorbs heat at low temperature from chilling water. The remaining liquid refrigerant is pressurized by refrigerant pump and vaporized in the generator using heat from the solar collector system, thus completing the cycle as shown in Fig. 1.

This work gives particular attention to the use of an ejector in the cooling cycle, due to it is construction simplicity, absence of moving parts, operation at low temperatures and a low operational cost, being attractive for refrigeration and air conditioning applications. It has been shown that the cooling cycle performance

* Corresponding author. Tel.: +56 61 207000; fax: +56 61 232284.
E-mail addresses: humberto.vidal@umag.cl (H. Vidal), colle@emc.ufsc.br (S. Colle).
[1] Tel.: +55 48 2342161; fax: +55 48 3317615.

1359-4311/$ - see front matter © 2005 Elsevier Ltd. All rights reserved.
doi:10.1016/j.applthermaleng.2005.09.012

Nomenclature

A	area (m^2)
COP	coefficient of performance of the thermally driven cycle (dimensionless)
c_p	specific heat of water (kJ/kg K)
C_r	ratio of heat capacities
c_{rl}	specific heat of refrigerant (kJ/kg K)
ECC	ejector cooling cycle
EV	expansion valve
f	solar fraction (dimensionless)
h	specific enthalpy (kJ/kg)
LMTD	logarithmic mean temperature difference
NTU	number of transfer units
$\dot{Q}_{aux}$	auxiliary burner heat transfer rate (kW)
$\dot{Q}_g$	generator heat transfer rate (kW)
$\dot{Q}_s$	solar heat transfer rate (kW)
$\dot{Q}_u$	useful solar heat (kW)
r_f	refrigerant mass ratio (dimensionless)
SHE	solar heat exchanger
T	temperature (°C)
T_o	return hot water temperature (°C)
T_f	refrigerant fluid temperature at the heat exchanger output (°C)
T_i	intermediate temperature (°C)
T_s	fluid temperature at the storage tank output (°C)
U	overall heat transfer coefficient (kW/m^2 K)
x	vapor quality
$\dot{\omega}_{ej}$	ejector primary mass flow rate (kg/s)
$\dot{\omega}_{ej\text{-}s}$	ejector secondary mass flow rate (kg/s)
W_{min}	minimum heat capacity (kW/K)
ε	heat exchanger effectiveness

Subscripts

amb	ambient
c	condenser, collector
e	evaporator
ev	evaporation
f	refrigerant fluid
g	generator
i	intermediate, inlet
l	liquid
lv	liquid–vapor
o	outlet
s	solar, sensible
sat	saturation
T	tilted
v	vapor, valve

depends on the design parameters of ejector and the operating conditions ($T_c, P_c, T_g, P_g, T_e, P_e$); these factors are related to the particular needs of the application [1]. The evaporation temperature T_e is usually in the range of 5–10 °C for air conditioning purposes and about −5 °C or −6 °C for refrigeration. The condensing temperature T_c depends both on the heat-rejecting equipment used for the condenser and on the type of the cooling fluid (water or air). For different climatic conditions T_c can vary over a wide range, usually 28–40 °C. The generation temperature, T_g is especially important to the solar ejector cooling system as it affects not only the ejector COP, but also the efficiency of the solar collector. An increase in T_g increases the COP but decreases the collector efficiency [2,3]. Increasing the condenser temperature above the design point (e.g., on a hot day) may lead to an unstable operation of the ejector, with COP decreasing rapidly. Further increases in condenser temperature will result in complete loss of ejector functioning.

The performance characteristics mentioned above and the solar-driven character of the ejector are reasons to

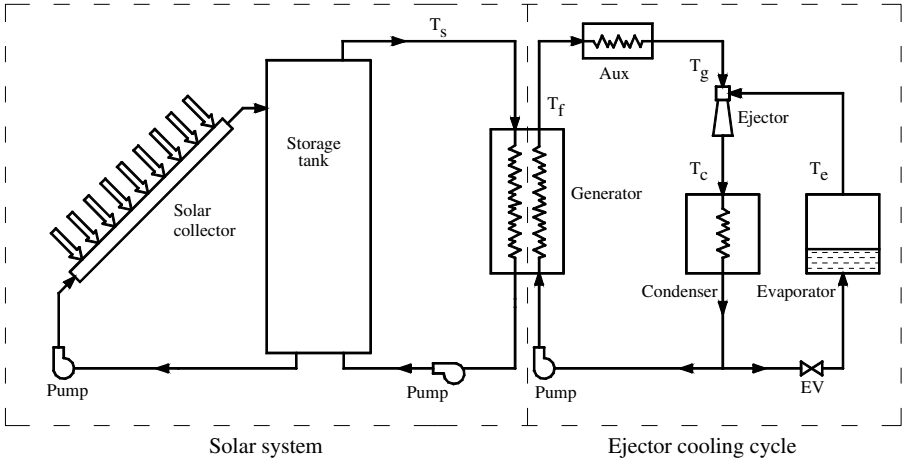

Fig. 1. Ejector cooling system assisted by solar energy.

simulate the solar ejector cooling system dynamically. Several research groups have studied the solar driven refrigeration system performance. In the case of solar absorption refrigeration systems, several works are found in the literature [4–6]. However, few computational models have been developed for solar ejector refrigeration systems. These models are also restricted not allowing to vary operation parameters due to climatic conditions and constant solar irradiation hypotheses is used [2,3,7,8]. Nevertheless, a dynamic simulation of a solar ejector cooling system with Butane as refrigerant fluid and using the TRNSYS-EES coupling is found in [9].

The main objective of this work is to develop a computational model to perform an hourly simulation of a solar ejector cooling system using R141b as the working fluid. For the simulation of the system, the well-known program TRNSYS [12] is used. However, the TRNSYS library has not an "ejector cooling cycle" component. In this case, a mathematical model developed by Huang et al. [1] representing the performance of a one-dimensional ejector is written in EES [13]. The information exchange between TRNSYS and EES is obtained using the TRNSYS component Type 66.

In the present study, R141b is selected as the working fluid for the ejector cooling cycle since this fluid is shown to be a good refrigerant for an ejector, as was found by [10,11]. Also, R141b has a positive-slope saturated-vapor line in the thermodynamic T–s diagram. Therefore, superheating is not as important as other working fluids. Additionally, R141b was used by Huang et al. [1] to verify experimentally the one-dimensional ejector model considered in the present work.

2. System description

TRNSYS is a computational program with a modular structure appropriate to simulate thermal energy systems with dynamic behavior. Each component is modeled using mathematical equations written in FORTRAN. Consequently, if some components of the system are not included in the TRNSYS library, their physical models can be programmed in FORTRAN, MATLAB, C++ or EES. The main components used in TRNSYS to model the solar ejector cooling system are shown in Fig. 2. A weather data file of a typical meteorological year for Florianópolis is used to model the long-term performance of the solar ejector refrigeration system. In [14], the authors have constructed the TMY considered a representative year for Florianópolis from a 10-years period of data. Using this approach, the long-term performance of the system can be evaluated and the system's dynamic behavior can be obtained. The monthly average daily radiation on a horizontal surface and monthly average ambient temperature corresponding to the referred database are presented in Fig. 3.

2.1. TRNSYS components modelling

The TRNSYS unit Type 66, allows the user to call an EES file, receive data from TRNSYS component ($T_s, \dot{\omega}_s$) and pass its output data to other TRNSYS component ($T_o, \mathrm{COP}, \dot{\omega}_s, f, \dot{Q}_{aux}$), as represented by Fig. 4(a). This component is used to host the EES program containing the model of ejector cooling cycle, called ECC. Initially, the mathematical model of the heat exchanger conjugated to the ejector cycle that represents a vapor generator with phase-change is presented.

2.1.1. Modelling of the generator heat exchanger conjugated to the ejector cycle

Fig. 4(b) shows the main components of the ejector cooling cycle: ejector, condenser, evaporator and vapor generator. The generator of the ejector cooling cycle connects solar and cooling cycle. This defines different

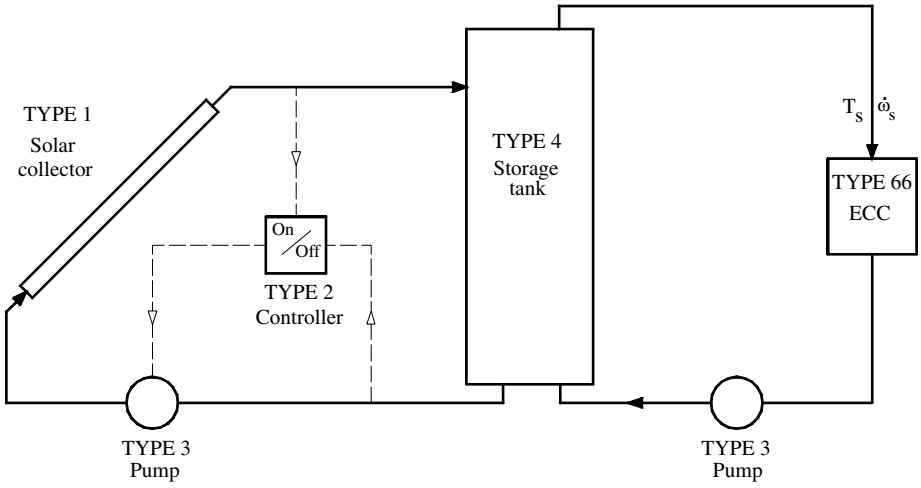

Fig. 2. Main components TRNSYS utilized in the simulation.

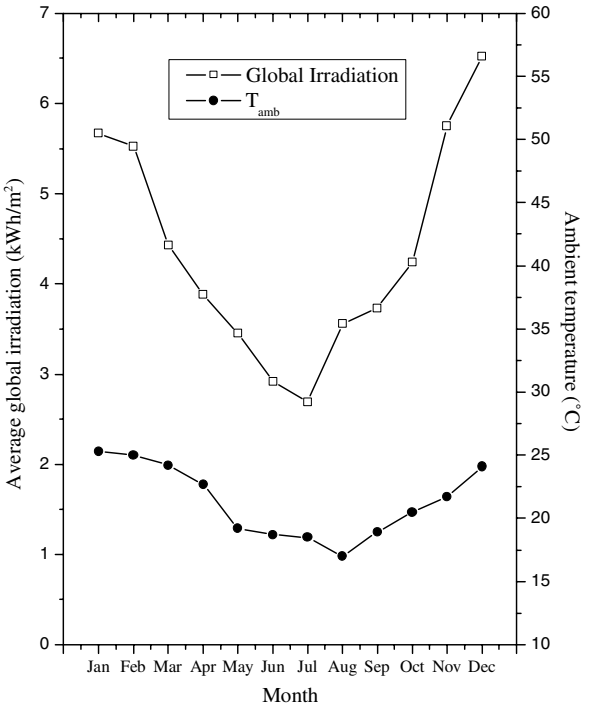

Fig. 3. Monthly average daily radiation and monthly average ambient temperature.

ways for heating the generator with the heat collected by the solar system. Three options are discussed in [15–17]. At the present work the configuration shown in Fig. 1 is chosen. In this configuration, the solar heat that drives the refrigeration system it is determined by the operation temperature, T_s (storage tank outlet) which depends on incident solar radiation and thermal losses. In simulation models found in the literature, T_s is set equal to T_f, meaning that the ideal heat exchange condition is assumed [2,3]. In other works [7,9,18], T_s is considered to be 10 °C higher than T_f. However, it should be noticed that the solar fraction f defined as $\dot{Q}_s/\dot{Q}_g$ will depend on the process of heat transfer with phase-change in the heat exchanger and therefore will also depend on the outlet refrigerant temperature, T_f. Additionally, if the refrigerant vapor does not reach the quality of saturated vapor, the presence of an auxiliary heater needs to be considered, as schematically presented in Fig. 4(b). The maximum $\dot{Q}_s$ to which solar fraction is unitary is $\dot{Q}_g = \dot{Q}_e/\mathrm{COP}$, where the COP is calculated to fixed and specified temperatures for the vapor flow in the generator, condenser and evaporator. In the heat transfer process of the ejector cycle generator, the temperature T_s varies with the energy gains and losses of the system and determines the different heat transfer regimes. The governing equations are developed in details in [19,20] and presented here as follows:

2.1.1.1. Case I: Sensible heat region ($T_f < T_g$). As shown in Fig. 5, the refrigerant fluid temperature T_f at the heat exchanger output is lower than the vapor generator temperature T_g. Therefore, the exchange is exclusively sensible heat and can be written as

$$\dot{Q}_s = W_{\min}\varepsilon_s(T_s - T_c) = \dot{\omega}_{ej}c_{rl}(T_f - T_c) \tag{1}$$

which is due to the heat exchanger effectiveness defined as

$$\varepsilon_s = \frac{\dot{\omega}_{ej}c_{rl}(T_f - T_c)}{W_{\min}(T_s - T_c)} \tag{2}$$

where

$$\varepsilon_s = \varepsilon_s\left(\frac{U_s A_s}{W_{\min}}\right)$$

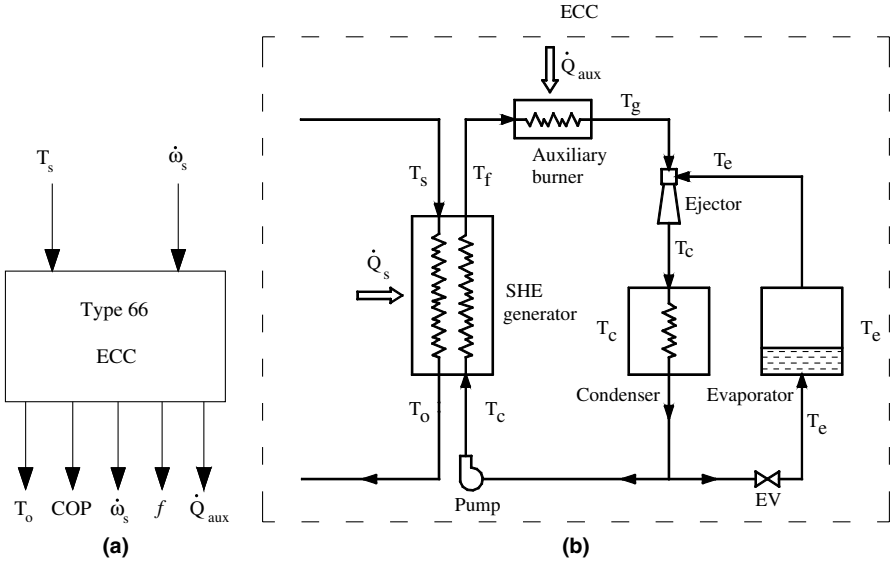

Fig. 4. (a) Component Type 66. (b) Ejector cooling cycle diagram.

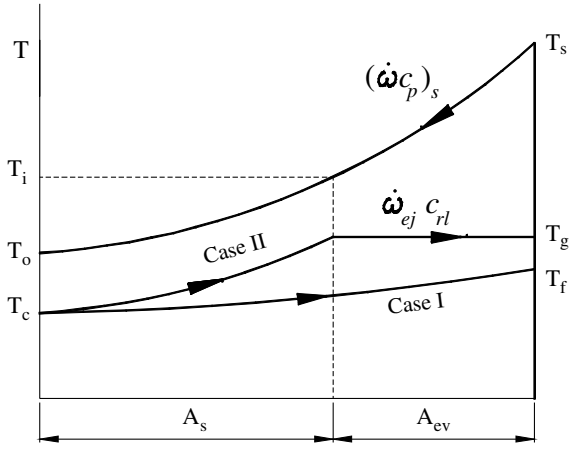

Fig. 5. Temperature distribution along the heat exchanger with phase-change.

A_s is the sensible exchanger area, $W_{min} = \min\{(\dot{\omega}c_p)_s, \dot{\omega}_{ej}c_{rl}\}$, $(\dot{\omega}c_p)_s$ being the heat capacity of the fluid by the solar system side, c_{rl} is the refrigerant specific heat at T_c and $\dot{\omega}_{ej}$ is the stationary mass flow in the vapor generator of the ejector cycle. The maximum value of T_s when $T_f = T_g$ is obtained from Eq. (1) and given by

$$T_{sl} = T_c + \frac{\dot{\omega}_{ej}c_{rl}(T_g - T_c)}{W_{min}\varepsilon_s} \tag{3}$$

If the temperature T_f is lower than T_g (and therefore T_s remains below T_{sl}), $\dot{Q}_s$ must be calculated by Eq. (1) as follows:

$$\dot{Q}_s = W_{min}\varepsilon_s(T_s - T_c) \tag{4}$$

The numerical process is continued until the temperature T_s reaches T_{sl} (or T_f reaches the temperature T_g). From Eq. (1), T_f results

$$T_f = T_c + \frac{\dot{Q}_s}{\dot{\omega}_{ej}c_{rl}} \tag{5}$$

2.1.1.2. Case II: Two-phase regime ($T_f = T_g$). Here, the refrigerant fluid experiences a phase-change for a particular heat exchange area, A_{ev} and the heat can be written as

$$\dot{Q}_s = \dot{\omega}_{ej}(h_f - h_c) \tag{6}$$

where $h_f = h_f(T = T_g, x = x_f)$, $h_c = h_c(T = T_c, x = 0)$ and x_f is the vapor quality of the refrigerant determined as follows:

In the sensible heat region, as shown in Fig. 5, the effectiveness is expressed by

$$\varepsilon_s = \varepsilon_s\left(\frac{U_sA_s}{W_{min}}\right) = \frac{\dot{\omega}_{ej}c_{rl}(T_g - T_c)}{W_{min}(T_i - T_c)} \tag{7}$$

where $A_s = A_{SHE} - A_{ev}$.

In the phase-change region, it can be seen that

$$\varepsilon_{ev} = \varepsilon_{ev}\left(\frac{U_{ev}A_{ev}}{(\dot{\omega}c_p)_s}\right) = \frac{(T_i - T_s)}{(T_g - T_s)} \tag{8}$$

where

$$\varepsilon_{ev} = 1 - \exp\left(\frac{-U_{ev}A_{ev}}{(\dot{\omega}c_p)_s}\right) \tag{9}$$

Eliminating T_i from Eqs. (7) and (8) leads to

$$T_c + \frac{\dot{\omega}_{ej}c_{rl}}{\varepsilon_s W_{min}}(T_g - T_c) = T_s + \varepsilon_{ev}(T_g - T_s) \tag{10}$$

From Eq. (6)

$$\begin{aligned} &h_f - h_c = h_l - h_c + h_{lv}x_f \\ &h_c = h_c(p_g, T_c), \quad p_g = p_{sat.}(T_g), \\ &h_l = h_l(T_g), \quad h_{lv} = h_{lv}(T_g) \end{aligned} \tag{11}$$

and from an energy balance in the phase-change region using the LMTD method one can show

$$(\mathrm{LMTD})_{ev}U_{ev}A_{ev} = \dot{\omega}_{ej}(h_f - h_l) = \dot{\omega}_{ej}h_{lv}x_f \tag{12}$$

Combining Eqs. (8) and (9), x_f can be determined by the following expression:

$$x_f = (T_g - T_c)(\dot{\omega}c_p)_s\left(\frac{\dot{\omega}_{ej}c_{rl}}{\varepsilon_s W_{min}} - 1\right) \times \left[1 - \exp\left(\frac{-U_{ev}A_{ev}}{(\dot{\omega}c_p)_s}\right)\right] \Big/ \dot{\omega}_{ej}h_{lv}\exp\left(\frac{-U_{ev}A_{ev}}{(\dot{\omega}c_p)_s}\right) \tag{13}$$

The hot water temperature of the solar system corresponding to the saturated vapor condition ($x_f = 1$), in the vapor generator output can be determined from Eq. (10)

$$T_{sv} = \left[T_c + \frac{\dot{\omega}_{ej}c_{rl}}{\varepsilon_s W_{min}}(T_g - T_c) - \varepsilon_{ev}T_g\right] \Big/ (1 - \varepsilon_{ev}) \tag{14}$$

The value of $\dot{\omega}_{ej}c_{rl}$ is assumed to be constant and specified by the ejector cooling cycle design considering a constant cooling capacity. When $T_s > T_{sv}$, the thermal capacity $(\dot{\omega}c_p)_s$ is controlled in order to ensure at all times saturated vapor condition in the vapor generator output. Using Eqs. (1) and (6), the return hot water temperature of the solar system can be determined by

$$T_o = T_s - \frac{\dot{Q}_s}{(\dot{\omega}c_p)_s} \tag{15}$$

2.1.2. Modelling of the ejector cooling cycle

2.1.2.1. Assumptions

- Steady-state operation.
- For the ejector performance analysis, the design calculation follows the method developed by Huang et al. [1].
- The geometric dimensions of the ejector are calculated according to refrigeration capacity and shown in Table 1.

- Pressure losses in all components and connecting pipes are negligible.
- Heat losses to the ambient are negligible except for the components exchanging energy with the environment.
- The working fluid R141b at the outlets of the generator, evaporator and ejector is considered saturated vapor.
- Condenser outlet is at saturated liquid state.
- The temperature rise across the circulation pump is negligible, (e.g., $h_4 = h_5$).
- The refrigerant properties are obtained directly from data bank of thermodynamic and transport properties built into EES.
- The expansion through the expansion valve is a throttling process, $h_4 = h_6$.
- Work supplied to the pump is neglected.
- A counter flow arrangement heat exchanger is considered and the effectiveness is given by

$$\varepsilon_s = \frac{1 - \exp[-\mathrm{NTU}(1 - C_r)]}{1 - C_r \exp[-\mathrm{NTU}(1 - C_r)]} \tag{16}$$

where $C_r = W_{min}/W_{max}$ and $\mathrm{NTU} = UA/W_{min}$.

Fig. 6(a) presents the schematic diagram of a typical ejector cooling cycle.

The thermodynamic cycle of the ejector cooling system can be illustrated by the P–h diagram shown in Fig. 6(b). The diagram must be carefully observed since for R141b, the slope of the vapor line in the P–h diagram on which points 1, 2 and 3 are, is smaller than the entropy slope.

For instance, assume that an ejector cooling cycle is designed to be operated at $T_g = 80\ ^\circ\mathrm{C}$, $T_c = 32\ ^\circ\mathrm{C}$, $T_e = 8\ ^\circ\mathrm{C}$, $\dot{\omega}_{ej} = 0.1054$ kg/s, for a cooling capacity $\dot{Q}_e = 10.5$ kW. From Fig. 6(b), the efficiency of an ejector cooling cycle can be represented by a thermal coefficient of performance derived as

$$\mathrm{COP} = \frac{\dot{Q}_e}{\dot{Q}_g} \tag{17}$$

where $\dot{Q}_e = \dot{\omega}_{ej\text{-}s}(h_2 - h_6)$ and $\dot{Q}_g = \dot{\omega}_{ej}(h_1 - h_5)$

$h_2 = h_2(T = T_e, x = 1)$; $\quad h_6 = h_4 = h_4(T = T_c, x = 0)$

$h_1 = h_1(T = T_g, x = 1)$; $\quad h_5 = h_4 = h_4(T = T_c, x = 0)$

Alternatively, Eq. (17) can be expressed as

$$\mathrm{COP} = \zeta \frac{h_2 - h_6}{h_1 - h_5} \tag{18}$$

Table 1
Ejector specification

Primary flow nozzle	
Throat diameter, mm	9.16
Exit diameter, mm	15.6
Constant-area section	Cylindrical type
Diameter, mm	22.5
Diffuser angle, deg	5

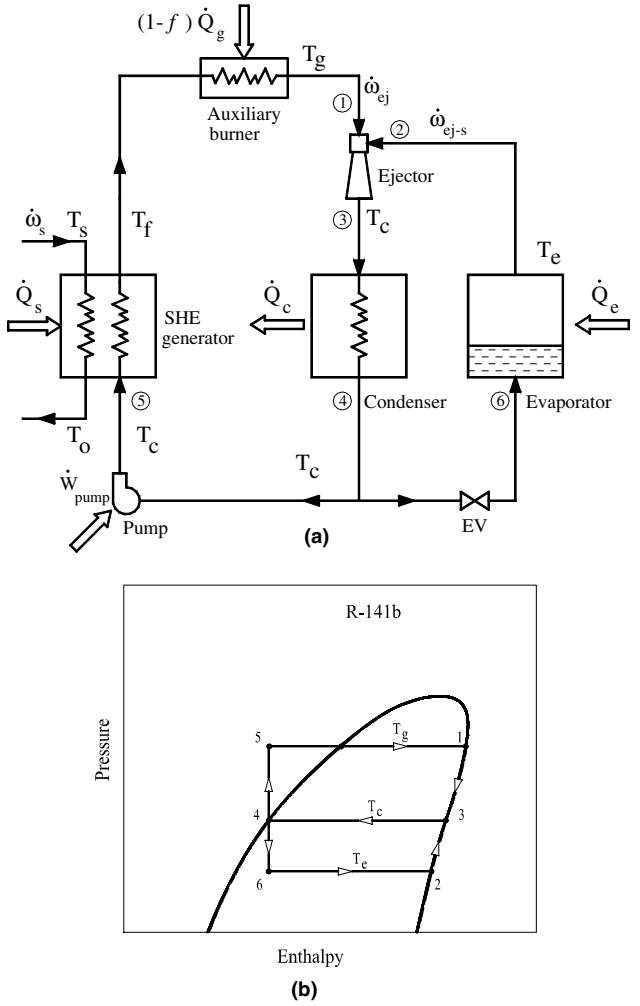

Fig. 6. (a) Schematic diagram of ejector cooling cycle with heat exchanger conjugated. (b) P–h diagram of the ejector cooling cycle.

where ζ is the entrainment ratio, defined as the ratio of secondary to primary vapor flow rates, $\dot{\omega}_{ej\text{-}s}$ and $\dot{\omega}_{ej}$, respectively.

The solar fraction f is defined as

$$f = \frac{\dot{Q}_s}{\dot{Q}_g} \tag{19}$$

where $\dot{Q}_s$ is calculated according to the heat exchange regime in the generator, explained in the cases I and II.

Once the solar fraction is known, the auxiliary heat can be evaluated by Eq. (20)

$$\dot{Q}_{aux} = (1 - f)\dot{Q}_g \tag{20}$$

2.2. TRNSYS components and operation parameters of the simulation

To construct the model, all the components of the system are interconnected in an appropriate manner to

represent the real system. The mathematical models for the system components are given in terms of their ordinary differential or algebraic equations and a brief description can be found in [12].

In order to simulate the dynamic behavior of a solar system, it is necessary to study such a system at an arbitrary short time step. A time step of 0.5 h was found to be convenient and reasonable for the simulation.

The solar ejector refrigeration system consists of:

(a) A data reader Type 9a used to read data from a file given by the user, making it available to other TRNSYS components at regular time intervals.
(b) A radiation processor Type 16a used to calculate several quantities related to the position of the sun and estimates radiation on a collector surface with slope and orientation specified.
(c) Flat plate collectors modelled with the Type 1b component. Two different solar collectors are selected to investigate the effect on the system performance [18]. Type I is a single glazed flat plate solar collector with a selective surface, and performance parameters $F_R U_L = 3.5\ \mathrm{W/m^2\ K}$, $F_R(\tau\alpha)_n = 0.8$. Type II is an evacuated-tube solar collector with tube-in-sheet fin with performance parameters $F_R U_L = 2.0\ \mathrm{W/m^2\ K}$, $F_R(\tau\alpha)_n = 0.8$.
(d) A storage tank, represented by the Type 4a, considered as fully mixed.
(e) Two heat collection circulating pumps modelled with the Type 3b component.
(f) An on/off controller for the circulating pump operating when the temperature difference across the collector array exceeds 10 °C and that stops when this difference is below 1 °C. This controller is modelled with the Type 2b component.
(g) A Type 66 TRNSYS component used to host the ejector's mathematical model programmed in EES and also to exchange information through the clipboard.
(h) A relief valve (component Type 13) used to release water vapor when the collector output water exceeds 98 °C and starts to boil.

2.2.1. Assumptions

1. The solar fraction is taken to be the part of the generator load that can be provided by the solar system. Power consumption by other equipment (circulating pump, fan motors and controllers) are excluded [4].
2. The mass flow rate per unit collector area is 50 kg/h m^2.
3. The storage tank is kept outdoors, since the daily average ambient temperature is higher than the indoor temperature, thus minimizing the energy loss from the storage tank [4].
4. The storage tank height is 2 m.

A schematic TRNSYS model of the solar ejector refrigeration system showing also the simulation program information flow is presented in Fig. 7.

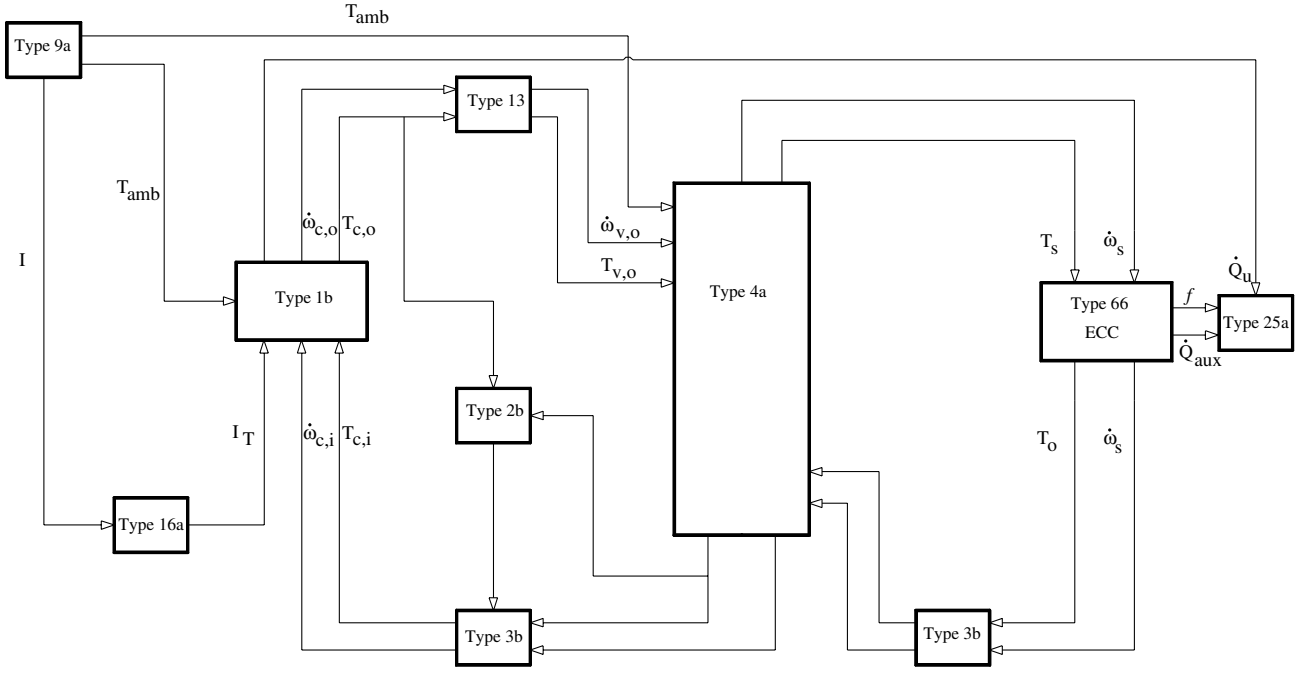

Fig. 7. TRNSYS model block diagram of the system.

3. System optimization

A large number of TRNSYS simulations were carried out to optimize the various factors affecting the performance of the solar ejector cooling system. Initially, the effect of the area and collector type is considered. The operation conditions of the ejector cooling cycle are prescribed as $T_g = 80\ °C$, $T_e = 8\ °C$, $T_c = 32\ °C$, COP = 0.39, $\dot{Q}_e = 10.5$ kW. The initial configuration of the solar subsystem consists of a 3 m^3 hot water storage tank, flat plate collector tilted 27° from the horizontal and a mass ratio $(\dot{\omega}_s/\dot{\omega}_{ej})$ equal to 8. Various collector areas between 20 and 140 m^2 are considered. The effect of the collector area is evaluated against the auxiliary heat required. As can be seen in Fig. 8(a), the greater the collector area lesser the auxiliary heat. This effect is amplified when using a more efficient solar collector (Type II).

The influence of the collector area on the heat gain is shown in Fig. 8(b). As expected, an increase in the collector area results in an increased collected heat. This effect is also amplified when a collector with better thermal quality is used.

The useful heat gain of the system for different storage tank volumes is presented in Fig. 9(a). It can be observed, that the increase in size of the storage tank above 2.5 m^3 slightly increases the collector heat gain. It should be noticed that, as the system operates during daytime while the radiation is proportional to the cooling load, the size of the storage tank does not significantly affect the system performance. Therefore, it is necessary to estimate the effect of storage tank volume size on the auxiliary energy consumption.

As can be seen in Fig. 9(b), the energy consumption by the auxiliary heater reaches a minimum value for

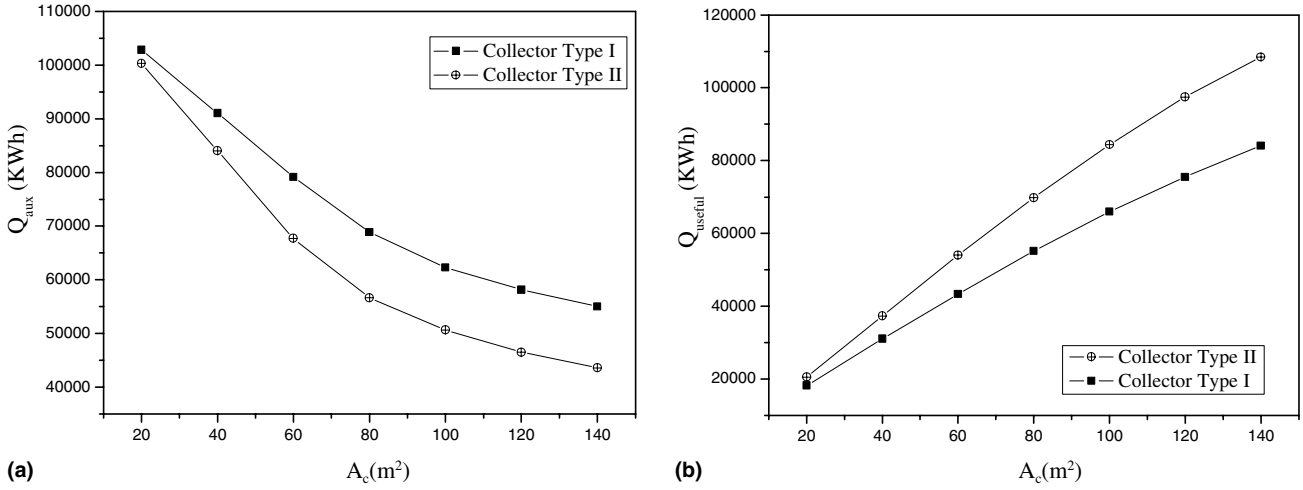

Fig. 8. (a) Effect of the collector area on the auxiliary heat required by the system. (b) Effect of the collector area on the collector useful heat gain.

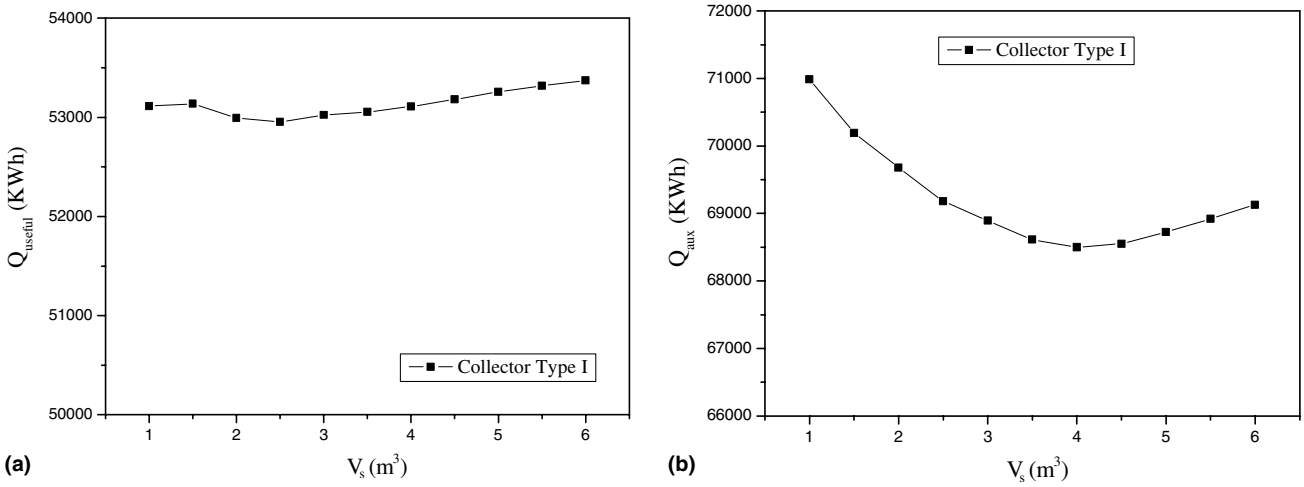

Fig. 9. (a) Effect of storage tank size on useful heat gain of the system. (b) Effect of storage tank size on auxiliary heat required by the system.

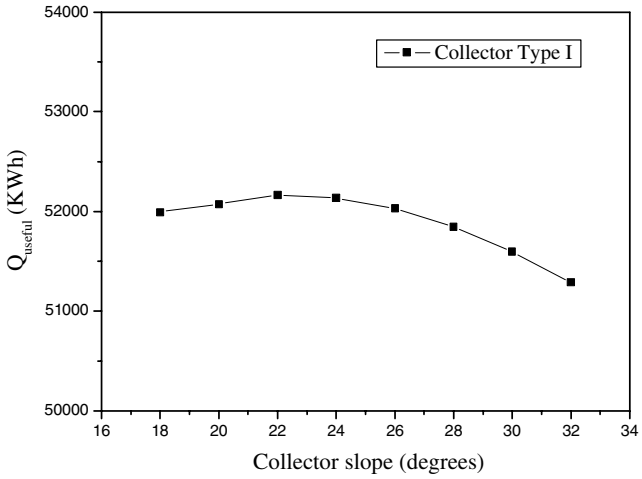

Fig. 10. Effect of collector slope angle on useful heat gain of the system (collector type I).

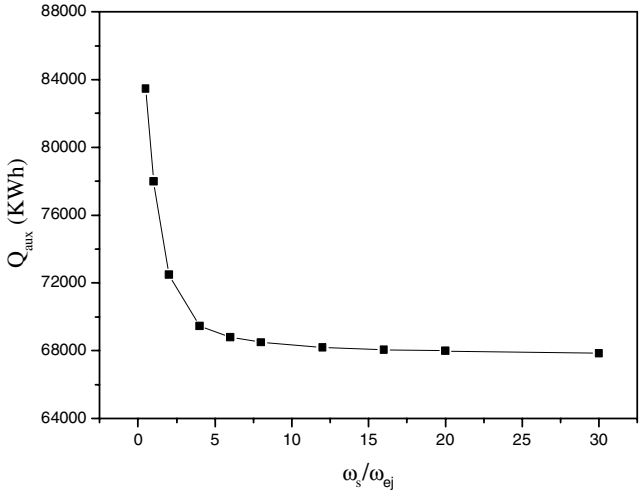

Fig. 11. Effect of the mass ratio on auxiliary heat of the system.

4 m^3 storage tank. Future works should also consider the model and the degree of stratification of the storage tank.

Simulations have shown that the solar heat gain from the system is not significantly affected for collector slope angles, as indicated in Fig. 10. However, the heat gain reaches the maximum value at a slope angle of 22° for the collector type I for Florianópolis (latitude 27°).

The effect of the mass ratio $r_f = (\dot{\omega}_s/\dot{\omega}_{ej})$ on the auxiliary heat consumption is shown in Fig. 11. As $\dot{\omega}_{ej}$ is considered to be constant in the ejector cooling cycle, an increase in r_f will be equivalent to an increase in the hot water flow of the solar system. A little increase in r_f at the interval between 0 and 6 (0 and 2278 kg/h hot water) decrease rapidly the auxiliary heat consumption. Successive increases above $r_f = 6$ does not affect the auxiliary heat consumption.

Fig. 12(a) shows the solar fraction for a particular case of the solar ejector cooling system. It can be observed that solar fraction reaches a minimum monthly value during July, thus matching the higher auxiliary energy consumption that occurs for the same month, as shown in Fig. 12(b).

4. Conclusions

A TRNSYS computational model of a solar ejector cooling system has been developed performing a parametric study to select the optimum system size. The model was used to investigate the effect of the area, slope and collector type, storage tank size and hot water flow rate on solar fraction, useful heat gain and auxiliary heat.

The annual auxiliary energy consumption decreases remarkably when the solar collector area increases from 20 to 80 m^2. However, the optimum solar collector area should be found by performing the life cycle cost

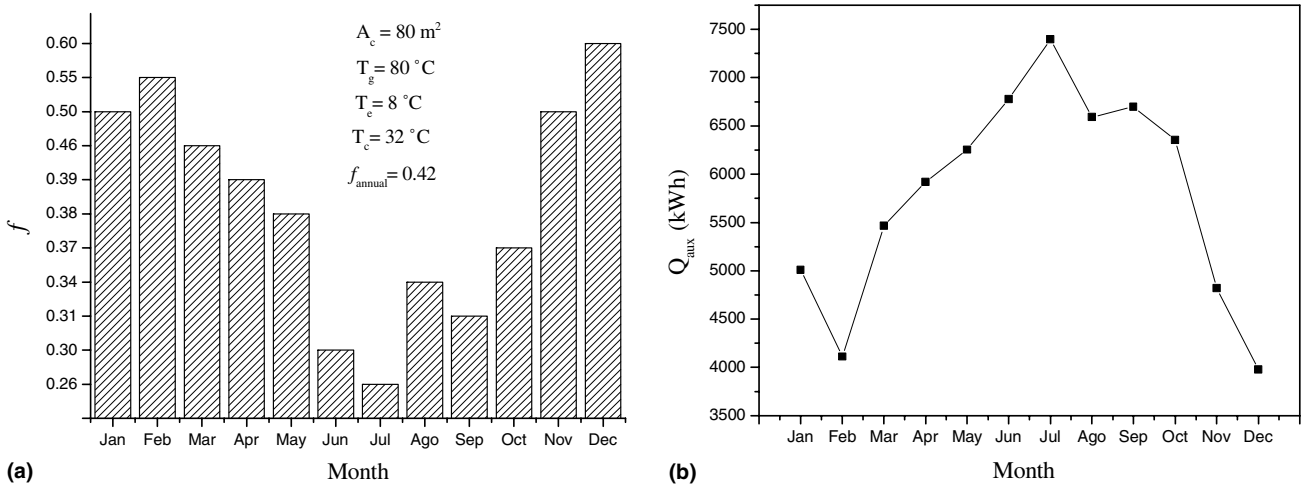

Fig. 12. (a) Monthly solar fraction of the solar ejector cooling system. (b) Monthly auxiliary heat consumption for the whole year.

analysis of the system. The size of the storage tank influences only slightly the useful heat gain of the system and has a greater effect on the auxiliary heat.

The final optimized system for a 10.5 kW cooling capacity consists of 80 m^2 of flat plate collector tilted 22° from the horizontal, a 4 m^3 hot water storage tank and a mass ratio equal to 8 resulting in a solar fraction of the system equal to 42% using the flat plate collector Type I.

This model allows the optimization of the various factors affecting the performance of the solar ejector cooling system and is potentially an effective tool to study the economical feasibility of the system.

References

[1] B.J. Huang, J.M. Chang, C.P. Wang, V.A. Petrenko, A 1-D analysis of ejector performance, International Journal of Refrigeration 22 (1999) 354–364.

[2] M. Sokolov, D. Hershgal, Solar-powered compression-enhanced ejector air conditioner, Solar Energy 51 (3) (1993) 183–194.

[3] A. Arbel, M. Sokolov, Revisiting solar-powered ejector air conditioner-the greener the better, Solar Energy 77 (1) (2004) 57–66.

[4] K.A. Joudi, J.Q. Abdul-Ghafour, Development of design charts for solar cooling systems, Part I: Computer simulation for a solar cooling system and development of solar cooling design charts, Energy Conversion & Management 44 (2003) 313–339.

[5] K. Sumathy, Z.F. LI, Simulation of a solar absorption air-conditioning system, Energy Conversion & Management 42 (2001) 313–327.

[6] G.A. Florides, S.A. Kalogirou, S.A. Tassou, L.C. Wrobel, Modelling and simulation of an absorption solar cooling system for Cyprus, Solar Energy 72 (2002) 43–51.

[7] B.J. Huang, J.M. Chang, V.A. Petrenko, K.B. Zhuk, Solar ejector cooling system using refrigerant R141b, Solar Energy 64 (4–6) (1998) 223–226.

[8] N.M. Khattab, M.H. Barakat, Modeling the design and performance characteristics of solar steam-jet cooling for comfort air conditioning, Solar Energy 73 (4) (2002) 257–267.

[9] W. Pridasawas, P. Lundquist, Optimization of a small-scale solar-driven ejector refrigeration system, in: Proceedings of EUROSUN, 14. Intern. Sonnenforum, Freiburg, Germany, paper no. 2-093-102, 2004.

[10] B.J. Huang, J.M. Chang, Empirical correlation for ejector design, International Journal of Refrigeration 22 (1999) 379–388.

[11] R. Dorantes, A. Lallemand, Prediction of performance of a jet cooling system operating with pure refrigerants or non-azeotropic mixtures, International Journal of Refrigeration 18 (1) (1995) 21–30.

[12] S.A. Klein, Trnsys 15: Reference manual 15, Solar Energy Laboratory—University of Wisconsin, Madison, 2000.

[13] S.A. Klein, F.L. Alvarado, EES-Engineering Equation Solver, F-Chart Software, Middletown, Wisconsin, 2001.

[14] S.L. Abreu, S. Colle, A.P. Almeida, S.L. Mantelli, Qualificação e recuperação de dados de radiação solar medidos em Florianópolis-SC, ENCIT 2000, 8th Brazilian Congress of Thermal Engineering and Sciences, October 2000, Brazil.

[15] K. Chunnanond, S. Aphornratana, Ejectors: applications in refrigeration technology, Renewable and Sustainable Energy Reviews 8 (2) (2004) 129–155.

[16] N.A. Shchetinina, S.Z. Zhadan, V.A. Petrenko, Comparison of the efficiency of various ways of heating the generator of a solar-ejector freon refrigerant machine, Geliotekhnika 23 (4) (1987) 71–74.

[17] D.W. Sun, I.W. Eames, Recent developments in the design theories and applications of ejectors—a review, Journal of the Institute of Energy 68 (1995) 65–79.

[18] B.J. Huang, V.A. Petrenko, I.YA. Samofatov, N.A. Shchetinina, Collector selection for solar ejector cooling system, Solar Energy 71 (4) (2001) 269–274.

[19] S. Colle, H. Vidal, G. Pereira, Limites de validade do método de projeto $f - \bar{\phi}$ chart para ciclos de refrigeração de ejetor assistidos por energia solar, Proceedings of VII Iberoamerican Congress of Solar Energy (CIES), September (2004), Vigo, Spain.

[20] S. Colle, H. Vidal, G. Pereira, Sistemas de refrigeração híbridos solar-gás natural por ciclo ejetor, Technical Report, CTPETRO Project No. 6504153016, Florianópolis, Brazil, 2004.